Time-Expanded Φ-OTDR Based on Binary Sequences

Javier Preciado-Garbayo, Miguel Soriano-Amat, Pascual Sevillano, David Izquierdo, Hugo F. Martins, Sonia Martin-Lopez, Miguel Gonzalez-Herraez, *Member, IEEE*, María R. Fernández-Ruiz, and Juan J. Martínez

***Abstract*— In this letter, the capabilities of time-expanded phase-sensitive optical time-domain reflectometry (TE Φ-OTDR) using binary sequences are demonstrated. We present a highly flexible and integrable TE Φ-OTDR approach that allows a customized distributed optical fiber sensor (range, spatial resolution, and acoustic sampling) by simply changing the length of the binary sequence and the reference clock frequencies of the binary sequence generators. The here presented architecture eliminates the need for the cumbersome arbitrary signal generators used to date to create the dual-comb spectra for interrogating the fiber. In this approach, the use of large binary sequences allows us to obtain dual combs in a simple and cost-effective way. Spatial resolution of ∼1 cm is achieved, attaining ∼15,000 independent measurements points along the interrogated fiber, with a capability of sensing ∼30,000 measurements points.**

***Index Terms*— Pseudo random binary sequences, structural health monitoring, time-expanded Φ-OTDR, Rayleigh scattering, dual frequency combs.**

Manuscript received May 8, 2022; revised June 1, 2022; accepted June 5, 2022. Date of publication June 9, 2022; date of current version June 17, 2022. This work was supported in part by the Spanish the Ministry of Science and Innovation (MICINN) through Grant RTC under Grant DI-17-09169, in part by Project Centro para el Desarrollo Tecnológico Industrial (CDTI) under Grant IDI 20210156, in part by the Comunidad de Madrid and FEDER Program under Grant P2018/NMT-4326, in part by the Spanish Government under Grant RTI2018–097957-B-C31/C33, in part by the Spanish Ministerio de Ciencia e Innovación (MCIN)/Agencia Estatal de Investigación (AEI) under Grant 10.13039/501100011033, and in part by the European Union Next Generation lan de Recuperación, Transformación y Resiliencia (EU-PRTR) Program through Project PSI under Grant PLEC2021-007875. The work of Miguel Soriano-Amat and María R. Fernández-Ruiz was supported by the Spanish MICINN under Contract PRE-2019–087444 and Contract IJC2018–035684-I. *(Corresponding author: Javier Preciado-Garbayo.)*

Javier Preciado-Garbayo is with the Aragon Photonics Laboratory (APL), 50009 Zaragoza, Spain, and also with the Electronic Engineering and Communications Department, EINA, University of Zaragoza, 50018 Zaragoza, Spain (e-mail: j.preciado@aragonphotonics.com).

Miguel Soriano-Amat, Sonia Martin-Lopez, Miguel Gonzalez-Herraez, and María R. Fernández-Ruiz are with the Departamento de Electrónica, Escuela Politécnica Superior, Universidad de Alcalá, 28805 Madrid, Spain (e-mail: miguel.soriano@uah.es; sonia.martinlo@uah.es; miguel.gonzalezh@uah.es; rosario.fernandezr@uah.es).

Pascual Sevillano is with the Aragon Institute of Engineering Research (I3A), Universidad de Zaragoza, 50018 Zaragoza, Spain (e-mail: psevi@unizar.es).

David Izquierdo is with the Centro Universitario de la Defensa (CUD), 50090 Zaragoza, Spain, and also with the Aragon Institute of Engineering Research (I3A), Universidad de Zaragoza, 50018 Zaragoza, Spain (e-mail: d.izquierdo@unizar.es).

Hugo F. Martins is with the Instituto de Óptica Daza de Valdés IO-CSIC, 28806 Madrid, Spain (e-mail: hugo.martins@csic.es).

Juan J. Martínez is with the Aragon Photonics Laboratory (APL), 50009 Zaragoza, Spain (e-mail: jj.martinez@aragonphotonics.com).

Color versions of one or more figures in this letter are available at https://doi.org/10.1109/LPT.2022.3181819.

Digital Object Identifier 10.1109/LPT.2022.3181819

I. Introduction

NOWADAYS, Distributed Optical Fiber Sensors (DOFS) are widely used for supervising large infrastructures (highways, pipelines or other civil structures) or environments by monitoring closely deployed optical fibers [1]–[3]. These technologies are capable of performing distributed measurements of physical changes along the fiber, such as strain, temperature, pressure, etc. DOFS are usually modelled as a continuous array of independent sensing points located along the fiber. Hence, DOFS have proven capable of measuring along ranges of tens of kilometers with spatial resolutions of a few meters, delivering well tens of thousands of sensing points. Such capacity, along with its long reach and the potential to use already deployed fibers makes DOFS a unique flexible and adaptive sensing solution.

Among the different techniques in the DOFS field, this work focuses on phase-sensitivity optical time domain reflectometry (Φ-OTDR), specifically, the recently proposed time-expanded technique. Time-expanded (TE) Φ-OTDR is a highly advantageous technique to perform distributed acoustic sensing with fine resolution (i.e., a few cm) over moderate ranges (usually below the kilometer), still maintaining the capacity of delivering tens of thousands of independent sensing points, as typical implementations of Φ-OTDR. In particular, the technique is characterized by requiring several orders of magnitude narrower detection and acquisition bandwidths than that corresponding to the attained spatial resolution in Φ-OTDR [4]. This performance is particularly interesting in applications related to structural health monitoring (SHM) [5]–[7], being the intellectual property of the technique already registered [8]. The novel technique is inspired by dual comb spectroscopy (DCS). It uses an electro-optically generated dual frequency comb (DFC) to perform a multiheterodyne detection of the backscattered traces in an otherwise typical Φ-OTDR scheme, aimed at obtaining a downconversion of the received optical signal to the RF domain. To overcome the trade-off between signal-to-noise ratio (SNR) and the peak-power limit to avoid nonlinear effects, the DFCs employed to date in TE Φ-OTDR have been based on phase spectral modulation of uniform-amplitude lines, thus avoiding the formation of low duty cycle train of pulses [4], [9]. Instead, the applied spectral phase modulation has guaranteed that the time domain envelope was spread along the period while the combs' optical bandwidth had a uniform, flat-top envelope spectrum. However, the generation of such a specific time-domain RF signals has required

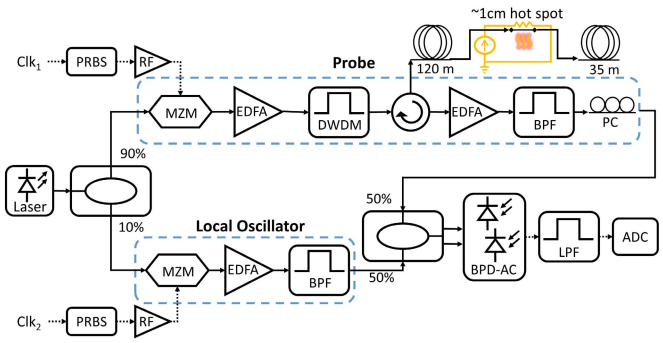

Fig. 1. Proposed TE Φ-OTDR architecture based on binary sequences. Two branches are used to generate the DFC, the upper one is to generate the probe signal the lower one generates the local oscillator. Acronyms are defined in the body of the manuscript.

the use of a high sampling rate arbitrary waveform generator (AWG). The added complexity in the comb generation scheme somehow blurs the relaxation in the detection process provided by TE Φ-OTDR.

In DCS, alternative methods to electro-optically (EO) generate a dual frequency comb have been proposed [10], [11]. In particular, it is possible to implement a spectral frequency comb avoiding the formation of low duty cycle pulses by using pseudo-random bit sequences (PRBS). Hence, inexpensive PRBS generation cards with certain tunability in the selection of the code length can readily substitute the cumbersome AWG in TE Φ-OTDR. The code length fixes the number of comb lines, N, which additionally corresponds to the number of independent sensing points delivered by the architecture, provided the whole available range is used. Besides, the use of PRBS cards delivers additional advantages, since it opens the door for the integration of the interrogator scheme, and offers complete freedom in the selection of the detuning between dual comb repetition rates, detaching this parameter from the memory depth available in an AWG. Note that the detuning in the combs' frequency rate has a minimum value given by the ratio between the AWG sampling rate and its memory depth [4]. Additionally, PRBS generators output higher power signals, reducing the demanding amplifiers or drivers before optical modulators. These characteristics of PRBS generators leads to a significant reduction in the cost, complexity and size of the TE Φ-OTDR interrogator system, being a key factor for their manufacturing and installation.

In this letter, we present and evaluate this simple, highly flexible and cost-effective solution for TE Φ-OTDR based on DFC allocated by PRBS generators. Using a 2^{15}-1 length PRBS sequence at ∼11 Gbps we demonstrate a spatial resolution of ∼1 cm with ∼15,000 independent measure points and ∼150 m sensing fiber length.

II. Materials and Methods

The proposed TE Φ-OTDR architecture to be used in the experimental demonstration is depicted in Fig. 1.

The optical source, a highly coherent continuous-wave laser with a linewidth <0.1 kHz, feeds two optical comb generators, one comb acting as the probe and the other as local oscillator (LO). Each comb generator is composed by a Mach-Zhender modulator (MZM) driven by a PRBS generation card that provides a deterministic and cyclic sequence of $N = 2^k - 1$ bits, where k is the order of the PRBS. These generators are based on a cascade of digital circuits with two possible states that change at the rate of the input clock. Therefore, the output signal in the temporal domain is a repetitive pattern whose bit time is set by the clock frequency. In the frequency domain, the spectrum depicts a comb that has a line spacing determined by the ratio between the clock rate and N, and whose amplitude is shaped by a sinc-like envelope. The clock signal for these generators was provided and controlled by two synchronized clock sources, Clk_1 and Clk_2. Once the frequency combs are obtained in the optical domain, they are boosted by an erbium-doped fiber amplifiers (EDFA) and filtered to reduce the amplified spontaneous emission (ASE) noise. The LO signal is filtered by a 12.5 GHz band pass filter (BPF) to suppress one sideband of the modulated signal and ensure a correct down-conversion in the detection. The probe signal is filtered with a 100 GHz bandwidth dense wavelength division multiplexer (DWDM). The optical power is adjusted in each branch with a variable optical attenuator (VOA). Then, the probe is coupled to a standard single mode fiber through a circulator. The backscattered signal from the fiber under test (FUT) is amplified and filtered by an EDFA and a 12.5 GHz BPF to keep the same sideband as the LO. Both single-sideband filtered signals are combined in a 50-50 coupler and detected with a 100 MHz bandwidth balanced AC detector (BPD-AC). The electrical received signal is low-pass filtered (LPF) with a 2 MHz cut-off frequency filter. The resulting electrical signal is acquired through a 10 MS/s analog-to-digital converter (ADC) for later processing. A polarization controller (PC) is included in the setup for alignment in order to maximize the sensitivity of the system.

The FUT is a 150 m long, as it was the available spool of that fitted the maximum range in our lab. The fiber is perturbed with a temperature stimulus obtained through a pair of 2 cm long metal wires parallel to the optical fiber and embedded into the optical fiber cable. The temperature variation is generated by a sinusoidal electrical signal of 0.2 Hz that allows the conductor to complete the thermal cooling-heating cycle without distortion. This configuration provides a stimulus whose effective length is ∼1 cm due to the heat dissipation along the extreme of the wires, having a Gaussian-like spatial distribution.

The measurement performance of the system is controlled by three parameters, the clock signal provided to one of the PRBS generators (f_{clk1}), the order of the cyclic PRBS (k) and the frequency difference between the clocks of probe and local oscillator ($\Delta f_{clk} = |f_{clk1} - f_{clk2}|$). The total bandwidth of the frequency comb (BW) is determined by the clock frequency, set to ∼11.1 GHz which yields to a nominal 0.9 cm resolution. The number of spectral lines in the frequency comb is directly set here by N. In our case, we set a 2^{15}-1 bit sequence which provides 32767 spectral lines and a frequency spacing ($f_r = BW/N$) between them of 340 kHz. These two parameters also define the maximum range, $c/(f_r 2n) = 304.26m$, where c is the speed of light in a vacuum and n is the refractive index of the fiber ($n = 1.45$); and the maximum acoustic

sampling $\delta f_{max} = f_r/2N = 5.17Hz$, where the acoustic sampling is fixed according to $\delta f = \Delta f_{clk}/N$. Finally, the Δf_{clk} will also be controlled by the clock generators and will settle the actual measurement conditions within the achievable range determined by BW and N which constrains its value to $\Delta f_{clk} < f_r/2$. This value also determines the compression factor, $CF = f_{clk1}/\Delta f_{clk}$, which accounts for the temporal expansion of the phase trace that loosens the requirements in the acquisition electronics.

Compared to the most common signal generator for the standard architecture, i.e., the AWG, PRBS generators are designed to test telecommunications system and thus higher bandwidths boards are not rare, which enables the use of higher frequency clocks and thus the increase of resolution of this proposed architecture. On the other hand, the sinc envelope originated by the temporal square shape of the bits implies an uneven power distribution among the spectral lines of the comb. Due to the relatively smooth edges of the optical BPF, some of the lower and higher frequency spectral lines are filtered out to prevent aliasing between Nyquist zones in RF domain. Furthermore, in the processing stage of the RF detected signal, high and low frequency lines of the comb in the first Nyquist zone are digitally filtered out according to their power spectral density in order to improve the SNR in the recovered phase trace. This yields to a reduction in the effective spectral lines and as consequences, the effective gauge length is slightly increased.

III. Results and Discussion

To demonstrate the validity of our proposal to perform high spatial resolution sensing, we apply a temperature stimulus as indicated in previous section. The probe signal optical power introduced to the FUT is 9 dBm, lower than the threshold for non-linear effects in the FUT as modulation instability (MI). The measured power of the backscattered signal is −25 dBm and the LO optical power before balanced detection is adjusted to −20 dBm, which is enough to perform the coherent detection while avoiding saturation in the detector. Once the optical signal is downconverted, it is sampled and processed. A conventional digital BPF is implemented to recover the first Nyquist zone [4]. Then the signal is transformed from the frequency domain to the time domain to recover the complex signal. Finally, the phase of the trace is demodulated and the detected phase changes are scaled to Celsius degrees according to [6]. Two different configurations of acoustic sampling rates, δf, i.e., 1 Hz and 5 Hz have been evaluated.

A. First Spectral Configuration (1 Hz)

In the first spectral configuration, the Δf_{clk} was configured so δf was set to 1 Hz, which yields to a CF of 340,000 and performs a time expansion from ∼1.4 μs to 500 ms. The effective gauge length in this configuration after a 23 kHz bandwidth digital filtering is set to ∼1.2 cm. Fig. 2 shows the power of the coherently detected traces acquired for 10 s, including an inset with a section of non-perturbed fiber. The overlapping of the traces confirms the phase stability of the measured signal for the time lapse. Fig. 3 shows the

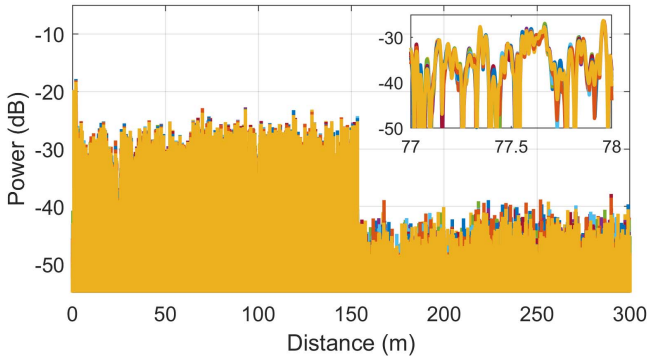

Fig. 2. Power of the coherently detected traces using δf of 1 Hz. Inset shows 10 s of an unperturbed section of consecutive acquired traces.

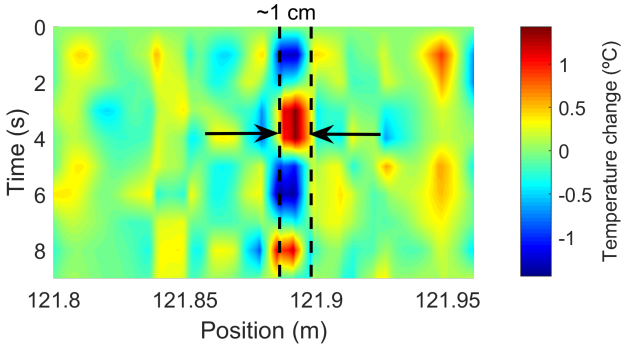

Fig. 3. Dynamic temperature map around the stimulated area.

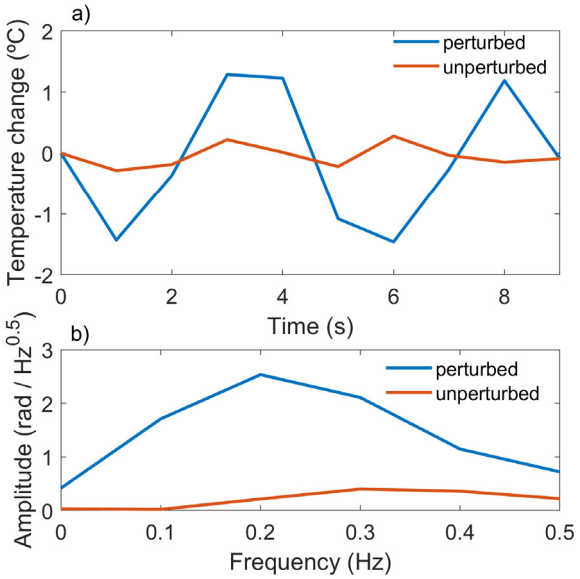

Fig. 4. a) The measurement of the temperature change in the stimulated area (blue) and at an unperturbed location (red). b) The ASD of each location.

temperature change map detected from the phase traces close the perturbed area.

In Fig. 4 a), a ∼2.5 °C peak-peak amplitude for the thermal stimulus is observed, and the measured phase change is ∼2 rad. The amplitude spectral density (ASD) of each location is shown in Fig. 4 b). The sensitivity based on

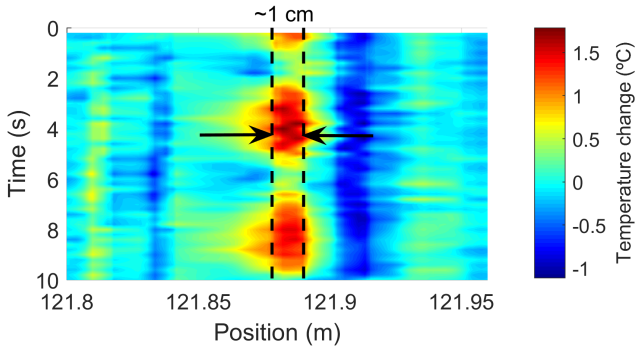

Fig. 5. Dynamic temperature map around the stimulated area.

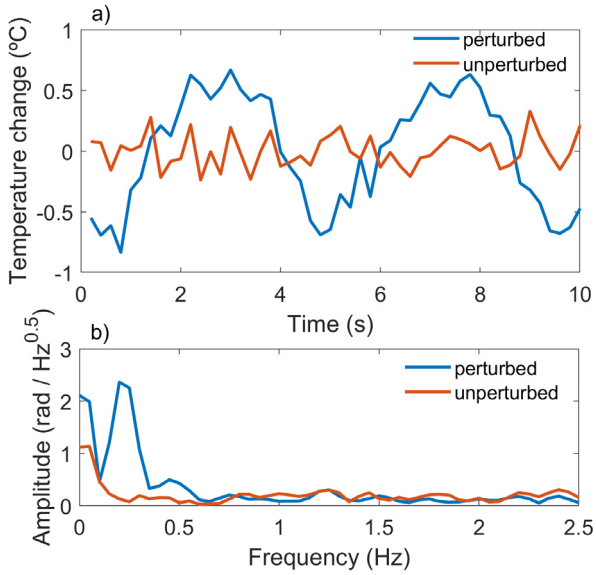

Fig. 6. a) The measurement of the temperature change in the stimulated area (blue) and at an unperturbed location (red). b) The ASD of each location.

the median standard deviation along the fiber in 1 s is 0.149 rad. In frequency domain, the ASD noise floor comes to 0.094 $rad/\sqrt{Hz}$ for this configuration. For the value of the gauge length employed in this case, the calculated temperature uncertainty is 0.142 °C.

B. Second Spectral Configuration (5 Hz)

In the second experiment, the Δf_{clk} was configured so δf was 5 Hz and the CF scaled to 68,000 which means that the sensed phase trace was expanded from ∼1.4 μs to 100 ms. Fig. 5 shows the temperature change map detected from the traces. The recovered measurement for the aforementioned stimulus with this configuration is depicted in Fig. 6 a), where a ∼1.5 °C peak-to-peak amplitude is observed. The ASD of each location is shown in Fig. 6 b).

Based on the measurement, the effective spatial resolution once the comb is filtered with a 62 kHz bandwidth filter reaches up to ∼2 cm. This increase in spatial resolution caused by the applied digital filtering explains that the perturbation appears wider in Fig. 5 with respect to the previous case (Fig. 3). The sensitivity, based on the median of the standard deviation for the phase values along the fiber in 1 s is 0.333 rad. Compared to the value obtained at 1 Hz, this value is consistent with the $\sqrt{5}$ degradation expected from the 5 times increase in acoustic bandwidth. On the frequency domain, the noise floor of the ASD shows a value of ∼0.098 $rad/\sqrt{Hz}$ along the measured fiber. However, in this case it is not consistent with the previous configuration, which can be explained due to additional low frequency noise in the ASD noise floor calculation that is out of band in the previous configuration. According to the effective gauge length obtained in this case, the calculated temperature uncertainty is 0.170 °C.

IV. Conclusion

We have presented a highly flexible architecture for TE Φ-OTDR based on the use of binary sequences that greatly reduces the complexity and requirements in the probe and local oscillator signal generation. The use of cyclic PRBS generators not only reduces the cost and complexity of the system but also increases the flexibility in the selection of DFC frequency offset, detaching the acoustic sampling rate of the measurement from the AWG memory depth availability. Besides, due to its common use in the telecommunications field, typical operating clock frequencies of 40 GHz and orders of $k = 31$ for the PRBS sequence are readily available and yield to fine resolution and long range performance values without costly electronics. Using the scheme here proposed, we have demonstrated a 1 cm resolution measurement and 0.142 °C accuracy with ∼15000 independent measurement points along ∼150 m fiber with a maximum achievable range of ∼300 m. This cost-effective and simple approach critically simplifies the interrogator integration process and opens the door for its use of this sensing technology in field test deployments.

References

[1] H. Wijaya, P. Rajeev, and E. Gad, "Distributed optical fibre sensor for infrastructure monitoring: Field applications," *Opt. Fiber Technol.*, vol. 64, Jul. 2021, Art. no. 102577.
[2] P. Lu *et al.*, "Distributed optical fiber sensing: Review and perspective," *Appl. Phys. Rev.*, vol. 6, no. 4, Sep. 2019, Art. no. 041302.
[3] X. Bao and L. Chen, "Recent progress in distributed fiber optic sensors," *Sensors*, vol. 12, no. 7, pp. 8601–8639, Jun. 2012.
[4] M. Soriano-Amat *et al.*, "Time-expanded phase-sensitive optical time-domain reflectometry," *Light, Sci. Appl.*, vol. 10, no. 1, pp. 1–12, Dec. 2021.
[5] M. Soriano-Amat *et al.*, "Monitoring of a highly flexible aircraft model wing using time-expanded phase-sensitive OTDR," *Sensors*, vol. 21, no. 11, pp. 1–10, 2021.
[6] Y. Koyamada, M. Imahama, K. Kubota, and K. Hogari, "Fiber-optic distributed strain and temperature sensing with very high measurand resolution over long range using coherent OTDR," *J. Lightw. Technol.*, vol. 27, no. 9, pp. 1142–1146, May 1, 2009.
[7] A. Barrias, J. R. Casas, and S. Villalba, "A review of distributed optical fiber sensors for civil engineering applications," *Sensors*, vol. 16, no. 748, pp. 1–35, 2016.
[8] H. F. Martins *et al.*, "Method and system for interrogating optical fibers," U.S. Patent 2021 0 364 385 A1, Nov. 25, 2021.
[9] M. Soriano-Amat, H. F. Martins, V. Durán, S. Martin-Lopez, M. Gonzalez-Herraez, and M. R. Fernández-Ruiz, "Quadratic phase coding for SNR improvement in time-expanded phase-sensitive OTDR," *Opt. Lett.*, vol. 46, no. 17, pp. 4406–4409, 2021.
[10] K. Fdil *et al.*, "Dual electro-optic frequency comb spectroscopy using pseudo-random modulation," *Opt. Lett.*, vol. 44, no. 17, p. 4415, 2019.
[11] N. B. Hébert, V. Michaud-Belleau, J. D. Anstie, J.-D. Deschênes, A. N. Luiten, and J. Genest, "Self-heterodyne interference spectroscopy using a comb generated by pseudo-random modulation," *Opt. Exp.*, vol. 23, no. 21, p. 27806, 2015.